Article

Discrete Photopatternable #-Conjugated Oligomers for Electrochromic Devices

Christian B. Nielsen, Alex Angerhofer, Khalil A. Abboud, and John R. Reynolds

J. Am. Chem. Soc., **2008**, 130 (30), 9734-9746 • DOI: 10.1021/ja7112273 • Publication Date (Web): 02 July 2008

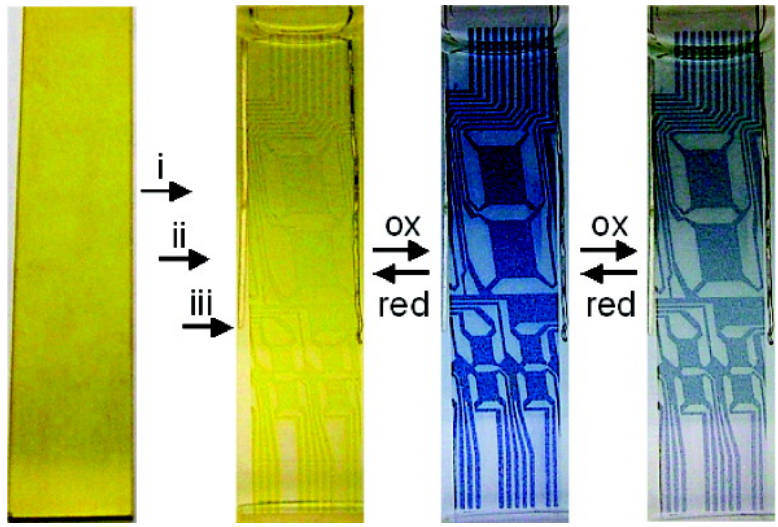

J|A|C|S
ARTICLES

Published on Web 07/02/2008

Discrete Photopatternable π-Conjugated Oligomers for Electrochromic Devices

Christian B. Nielsen, Alex Angerhofer, Khalil A. Abboud, and John R. Reynolds*

The George and Josephine Butler Polymer Research Laboratory, Department of Chemistry, Center for Macromolecular Science and Engineering, University of Florida, Gainesville, Florida 32611

Received January 4, 2008; E-mail: reynolds@chem.ufl.edu

Abstract: Three discrete oligomeric systems including an all-thiophene (**T6**) system, a thiophene/phenylene (**TPTTPT**) system, and a thiophene/EDOT/phenylene (**TPEEPT**) system have been constructed and characterized with emphasis on structural, optical, electrochemical, and spectroelectrochemical properties. For all three chromophores, the radical cation, the dication, and the π-dimer have been identified and characterized. EPR spectroscopy reveals that the radical cations of **TPTTPT** and **TPEEPT** have *g* values of 2.008−2.012 and peak-to-peak widths in the range 4.2−5.3 G. Formation of the radical cation takes place at a lower potential for **TPEEPT** than for **TPTTPT** and **T6**, whereas subsequent oxidation to the dication occurs more easily for **TPTTPT** than for **TPEEPT** and **T6**. We ascribe this observation to more localized charges in the oxidized species of **TPEEPT**, which is supported by our finding that the radical cation of **TPEEPT** is less prone to undergo π-dimerization than the radical cations of **TPTTPT** and **T6**. All the oxidized species are sufficiently stable to allow for optical characterization, and the relative positions of all absorption bands are found to be in agreement with the electrochemical data. For further solid-state modifications of these materials, we have effectively modified the synthetic design and grafted terminal functionalities (e.s. acrylates) onto the discrete oligomers. Of these novel materials, **TPEEPT** proves to be the most promising anodically coloring material for electrochromics, and it undergoes reversible switching between two different colored states (bright yellow and clear blue) and one almost transparent and color neutral state. Contrast ratios, measured as $\Delta\%T$ at λ_{max}, are as high as 62.5%, and switching times are in the range 2−5 s for the coloration process, though significantly longer for the bleaching process. As a proof of concept, we have successfully constructed a simple photopatterned electrochromic device by exploiting the terminal acrylate functionalities of the oligomers in a UV-initiated cross-linking process. To the best of our knowledge, this is the first oligomer-based photopatterned electrochromic device reported in the literature.

Introduction

Ever since the discovery of electrical conductivity in doped polyacetylene, extensive research has been focused on new conjugated materials, their design, synthesis, and application in electronic devices.[1] This class of materials primarily includes a vast number of conjugated polymers, but also more well-defined systems such as dendrimers and discrete oligomers.[2–6] Considering the discrete π-conjugated oligomers, they not only serve as important model compounds for understanding fundamental properties of π-conjugated polymers, but also have been shown to possess attractive properties themselves for application in electroactive devices such as organic field-effect transistors,[7–12] organic light-emitting diodes,[13–16] and in photovoltaic devices, either on their own or as part of a donor−acceptor system with fullerenes.[17–20] The major advantage of discrete oligomers

(1) Shirakawa, H.; Louis, E. J.; MacDiarmid, A. G.; Chiang, C. K.; Heeger, A. J. *J. Chem. Soc., Chem. Commun.* **1977**, *1977*, 578–580.
(2) Lo, S. C.; Burn, P. L. *Chem. Rev.* **2007**, *107*, 1097–1116.
(3) Mullen, K.; Wegner, G. *Electronic Materials: The Oligomer Approach*; Wiley-VCH: Weinheim, Germany, 1998.
(4) Martin, R. E.; Diederich, F. *Angew. Chem., Int. Ed.* **1999**, *38*, 1350–1377.
(5) Fichou, D. *J. Mater. Chem.* **2000**, *10*, 571–588.
(6) Skotheim, T. A.; Reynolds, J. R. *Handbook of Conducting Polymers*; Marcel Dekker: New York, 2007.
(7) Facchetti, A.; Deng, Y.; Wang, A. C.; Koide, Y.; Sirringhaus, H.; Marks, T. J.; Friend, R. H. *Angew. Chem., Int. Ed.* **2000**, *39*, 4547–4551.
(8) Yoon, M. H.; Facchetti, A.; Stern, C. E.; Marks, T. J. *J. Am. Chem. Soc.* **2006**, *128*, 5792–5801.
(9) Murphy, A. R.; Frechet, J. M. J. *Chem. Rev.* **2007**, *107*, 1066–1096.
(10) Horowitz, G.; Fichou, D.; Peng, X. Z.; Xu, Z. G.; Garnier, F. *Solid State Commun.* **1989**, *72*, 381–384.
(11) Dodabalapur, A.; Torsi, L.; Katz, H. E. *Science* **1995**, *268*, 270–271.
(12) Dimitrakopoulos, C. D.; Purushothaman, S.; Kymissis, J.; Callegari, A.; Shaw, J. M. *Science* **1999**, *283*, 822–824.
(13) Geiger, F.; Stoldt, M.; Schweizer, H.; Bauerle, P.; Umbach, E. *Adv. Mater.* **1993**, *5*, 922–925.
(14) Gigli, G.; Barbarella, G.; Favaretto, L.; Cacialli, F.; Cingolani, R. *Appl. Phys. Lett.* **1999**, *75*, 439–441.
(15) Mitschke, U.; Bauerle, P. *J. Mater. Chem.* **2000**, *10*, 1471–1507.
(16) Hung, L. S.; Chen, C. H. *Mater. Sci. Eng., R* **2002**, *39*, 143–222.
(17) Jorgensen, M.; Krebs, F. C. *J. Org. Chem.* **2004**, *69*, 6688–6696.
(18) Huisman, C. L.; Huijser, A.; Donker, H.; Schoonman, J.; Goossens, A. *Macromolecules* **2004**, *37*, 5557–5564.
(19) Otsubo, T.; Aso, Y.; Takimiya, K. *J. Mater. Chem.* **2002**, *12*, 2565–2575.

10.1021/ja7112273 CCC: $40.75

compared to their polymeric counterparts is monodispersity and hence a more direct and unambiguous correlation between structure and properties. From a synthetic point of view, the synthesis of discrete oligomers will often be more tedious and time-consuming than synthesis of conjugated polymers. However, structural complexity, such as incorporation of reactive end groups, can often be more easily achieved for well-defined oligomers than for polymers as a consequence of the different synthetic approaches.

Here, we report on a new family of discrete conjugated oligomers and their electrochromic properties. Whereas conjugated polymers (e.g., polyanilines, polypyrroles, and polythiophenes), which have been used widely for electrochromic applications,[21–26] generally have broad electronic absorption bands, discrete oligomers have more narrow and well-defined electronic absorption bands and are thus expected to undergo more clear and distinct color changes during the redox processes exploited for electrochromic behavior. This has been investigated nicely by Shirota and co-workers, who have reported on the electrochromic behavior of several polymeric systems containing small isolated chromophores.[27–29] By attaching conjugated oligomers of varying length to vinyl and methacrylate polymers as pendant groups, they were able to create several electrochromes, which all underwent clear and reversible color changes (i.e., from blue to pale yellow, green to yellow, and orange to purple) upon oxidation. Similar systems have been described by other researchers including Barbarella and co-workers and Ferraris and co-workers.[30,31] As opposed to attaching the isolated chromophores as a pendant group, they can also be incorporated into a polymer backbone using one of several approaches. As one example, McCulloch and co-workers have illustrated this well by synthesizing liquid crystalline organic semiconductors with photopolymerizable end groups;[32,33] the isolated chromophores could thus be incorporated into a highly ordered cross-linked network by UV-curing subsequent to film processing.

Inspired by several of the aforementioned contributions to recent advances in electrochromism and oligomer design and processing, we have recently taken interest in new π-conjugated materials that encompass the desired electroactive properties, processability, and stability and also provide an opportunity to incorporate the π-conjugated system covalently into a more complex macromolecular system. As illustrated in Figure 1A, we have been focusing on a series of discrete oligomers with an overall coil−rod−coil structure consisting of two alkyl spacers and a central π-conjugated oligomer segment. By adding terminal acrylate functionalities, we aim to exploit the self-organizing capability of the system induced by π-stacking between neighboring π-conjugated segments during processing (Figure 1B) and to introduce a second degree of connectivity by photoinduced cross-linking at the termini as depicted in a simplified manner in Figure 1C. Because of the extended connectivity, the soluble π-conjugated material is converted into an insoluble cross-linked structure. Moreover, if the cross-linking takes place without disrupting the intermolecular ordering and the electroactive properties drastically, then this approach can be used for photopatterning of optoelectronic devices with cooperative interactions between chromophores.

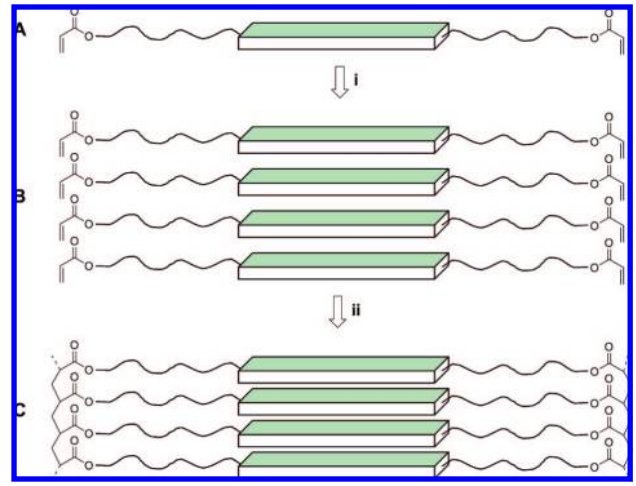

Figure 1. Schematic illustration of the idealized concept of processing (i) of telechelic oligomers (A) to create π-stacked domains (B) that can be further modified by photoinduced cross-linking (ii) to give cross-linked networks (C).

This strategy has thus far resulted in the design of three new thiophene- and phenylene-based oligomeric systems, and we present here the synthesis and characterization of these oligomers as well as our work toward photopatterning and electrochromic display fabrication.

Oligomer Synthesis and Characterization

Synthesis of Model Oligomers. To establish the fundamental properties of the π-conjugated segments of the target compounds, we initially synthesized the two model compounds **TPTTPT-Me$_2$** and **TPEEPT-Me$_2$** (**T** for thiophene, **P** for phenylene, and **E** for EDOT), as depicted in Scheme 1.[34]

1,4-Dibromo-2,5-bis(dodecyloxy)benzene was converted to the 1-aryl-4-bromo-2,5-bis(dodecyloxy)benzenes **1** and **3** via Stille couplings with the appropriate 2-stannylated thiophenes using stoichiometric imbalance to ensure dominant monoreaction. Subsequent Negishi couplings with 2-chlorozinc-5-methylthiophene afforded the monomethylated bisthienylbenzenes

(20) Segura, J. L.; Martin, N.; Guldi, D. M. *Chem. Soc. Rev.* **2005**, *34*, 31–47.
(21) Argun, A. A.; Aubert, P. H.; Thompson, B. C.; Schwendeman, I.; Gaupp, C. L.; Hwang, J.; Pinto, N. J.; Tanner, D. B.; MacDiarmid, A. G.; Reynolds, J. R. *Chem. Mater.* **2004**, *16*, 4401–4412.
(22) Garnier, F.; Tourillon, G.; Gazard, M.; Dubois, J. C. *J. Electroanal. Chem.* **1983**, *148*, 299–303.
(23) Hyodo, K. *Electrochim. Acta* **1994**, *39*, 265–272.
(24) (a) Mortimer, R. J.; Dyer, A. L.; Reynolds, J. R. *Displays* **2006**, *27*, 2–18. (b) Dyer, A. L.; Reynolds, J. R. In *Handbook of Conducting Polymers*, 3rd ed.; Skotheim, T. A., Reynolds, J. R., Eds.; CRC Press: Boca Raton, FL, 2007.
(25) Sapp, S. A.; Sotzing, G. A.; Reynolds, J. R. *Chem. Mater.* **1998**, *10*, 2101–2108.
(26) Thompson, B. C.; Kim, Y. G.; McCarley, T. D.; Reynolds, J. R. *J. Am. Chem. Soc.* **2006**, *128*, 12714–12725.
(27) Ohsedo, Y.; Imae, I.; Shirota, Y. *J. Polym. Sci., Part B: Polym. Phys.* **2003**, *41*, 2471–2484.
(28) Shirota, Y. *J. Mater. Chem.* **2000**, *10*, 1–25.
(29) Nawa, K.; Miyawaki, K.; Imae, I.; Noma, N.; Shirota, Y. *J. Mater. Chem.* **1993**, *3*, 113–114.
(30) Melucci, M.; Barbarella, G.; Zambianchi, M.; Benzi, M.; Biscarini, F.; Cavallini, M.; Bongini, A.; Fabbroni, S.; Mazzeo, M.; Anni, M.; Gigli, G. *Macromolecules* **2004**, *37*, 5692–5702.
(31) Meeker, D. L.; Mudigonda, D. S. K.; Osborn, J. M.; Loveday, D. C.; Ferraris, J. P. *Macromolecules* **1998**, *31*, 2943–2946.
(32) McCulloch, I.; Zhang, W. M.; Heeney, M.; Bailey, C.; Giles, M.; Graham, D.; Shkunov, M.; Sparrowe, D.; Tierney, S. *J. Mater. Chem.* **2003**, *13*, 2436–2444.
(33) McCulloch, I.; Bailey, C.; Genevicius, K.; Heeney, M.; Shkunov, M.; Sparrowe, D.; Tierney, S.; Zhang, W. M.; Baldwin, R.; Kreouzis, T.; Andreasen, J. W.; Breiby, D. W.; Nielsen, M. M. *Philos. Trans. R. Soc. London, Ser. A* **2006**, *364*, 2779–2787.
(34) Wan, J. H.; Feng, J. C.; Wen, G. A.; Wang, H. Y.; Fan, Q. L.; Wei, W.; Huang, C. H.; Huang, W. *Tetrahedron Lett.* **2006**, *47*, 2829–2833.

Scheme 1

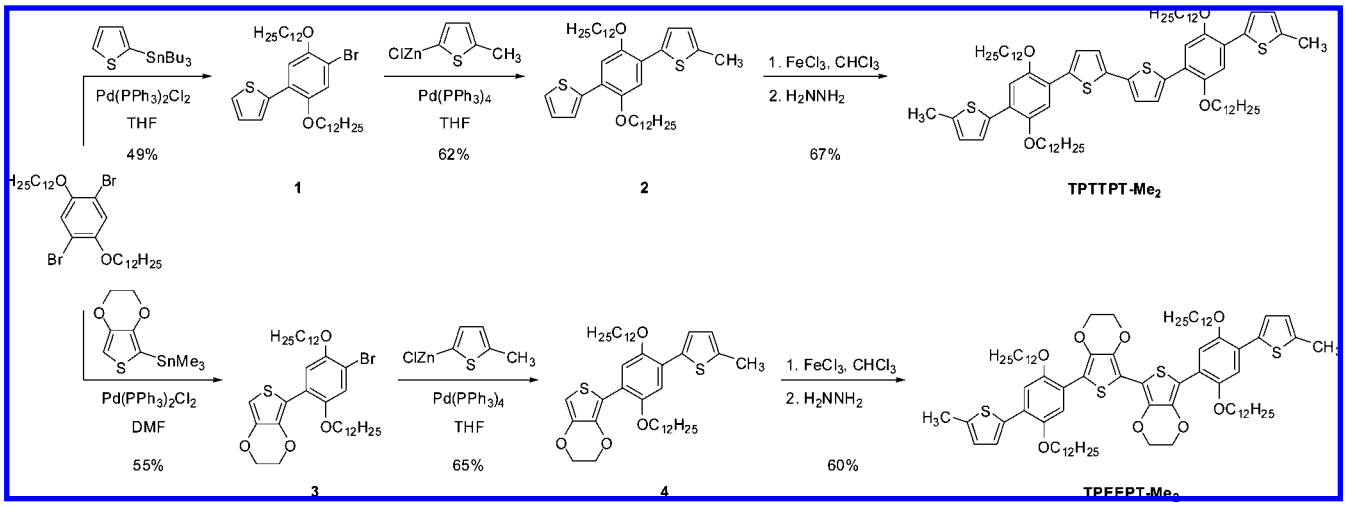

2 and **4**, which were then oxidatively homocoupled to give **TPTTPT-Me$_2$** and **TPEEPT-Me$_2$** in good yields.

Structural Analysis. For X-ray diffraction studies, single crystals of **TPTTPT-Me$_2$** and **TPEEPT-Me$_2$** were grown, but unfortunately, all crystallization experiments afforded crystals that were not suitable for structural analysis. Instead, the model compounds **PTTP** and **PEEP** depicted in Figure 2 were designed to resemble the central conjugated moieties of **TPTTPT-Me$_2$** and **TPEEPT-Me$_2$**, respectively. These model compounds were synthesized using a similar method (Supporting Information), and suitable single crystals were successfully obtained by slow evaporation of a dichloromethane/hexane mixture (**PTTP**) and a dichloromethane/acetonitrile mixture (**PEEP**).

The crystal structures of **PTTP** and **PEEP** are displayed in Figures 3 and 4. Both molecules are located on inversion centers and have a completely planar central bithiophene moiety in the anti configuration. For **PTTP**, the outer phenyl rings are twisted out of the plane by 24.4(7)° relative to the inner thiophenes; favorable S−O interactions are evident from an intramolecular S−O distance of 2.747(1) Å, which is significantly shorter than the sum of the van der Waals radii (3.35 Å).[35,36] Single crystals of **PEEP** adapt an even more coplanar structure with a dihedral angle between the inner thiophene and the outer phenyl ring of only 8.0(2)°; S−O distances of 2.899(2) Å between the two EDOT rings and 2.627(2) Å between the alkoxy group and the thiophene again demonstrate highly favorable S−O interactions, which most likely contribute greatly to the coplanar arrangement. Furthermore, we note that the four dodecyl side chains in **PEEP** exhibit an all-trans configuration and are nearly coplanar to the aromatic core.

Synthesis of Telechelic Oligomers. The synthesis of telechelic oligomers with identical conjugated backbones as the model compounds (Scheme 2) was achieved using a similar approach as described for the model oligomers above. Starting from the protected 6-(2-thienyl)-1-hexanol (**5**), which was easily synthesized from the corresponding bromide and 2-lithiothiophene, a Negishi coupling with either **1** or **3** afforded the monofunctionalized bisthienobenzenes **6** and **8**. In this instance, homocoupling was carried out by lithiation and subsequent treatment with ferric acetylacetonate, since the previously applied ferric chloride conditions were incompatible with the hydroxyl protection group.[37] Deprotection of **7** and **9** were easily achieved under mildly acidic conditions to give the functional oligomers **TPTTPT-diol** and **TPEEPT-diol** in excellent yields; further modification of the terminal hydroxy functionality with acryloyl chloride afforded **TPTTPT-diacrylate** and **TPEEPT-diacrylate**.

Additionally, an all-thiophene oligomer was synthesized as described in Scheme 3. The dialkylated quaterthiophene **10** was dibrominated (**11**) and then successfully converted to the

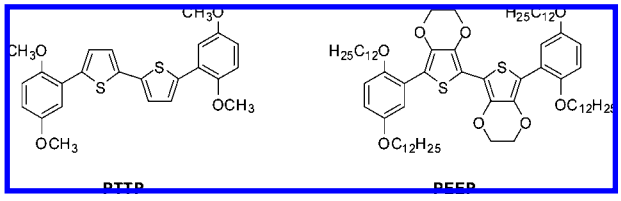

Figure 2. Structure of model compounds **PTTP** and **PEEP**.

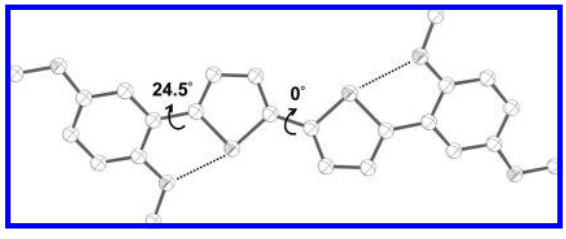

Figure 3. Molecular structure of a **PTTP** single crystal.

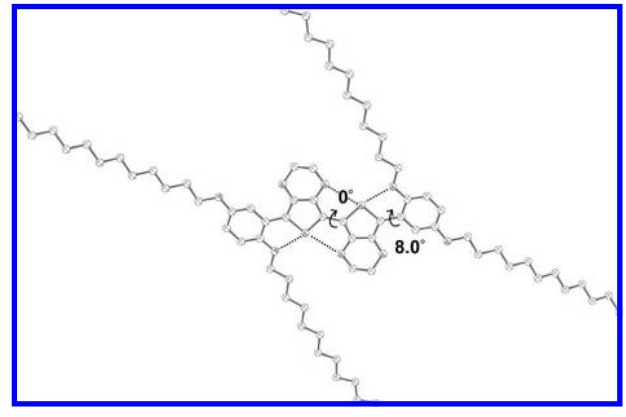

Figure 4. Molecular structure of a **PEEP** single crystal.

Scheme 2

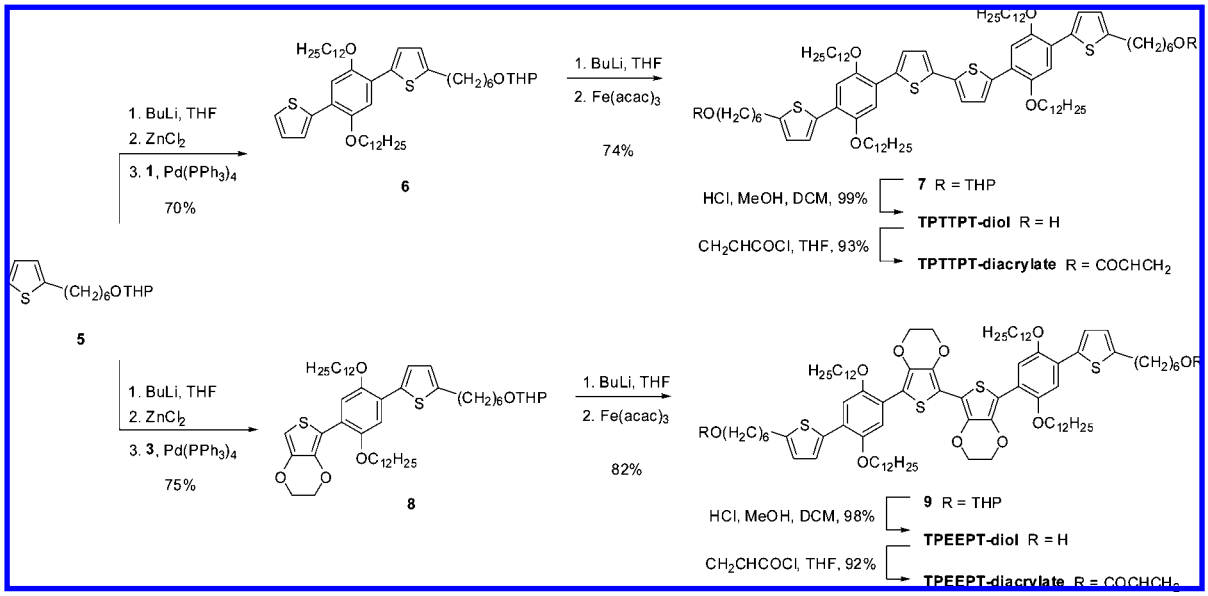

Scheme 3

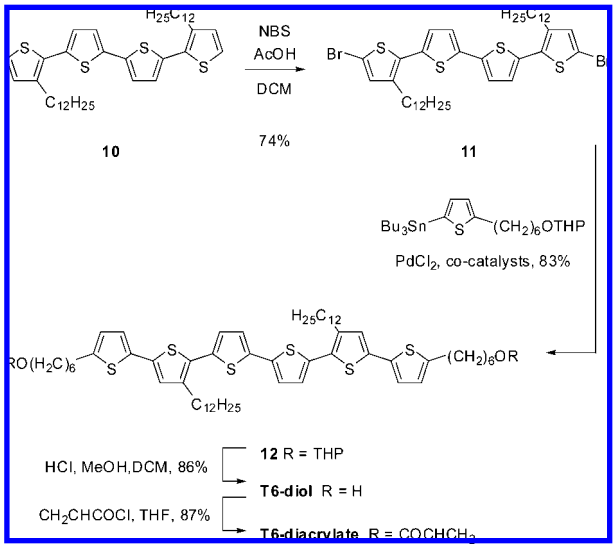

sexithiophene **12** in high yield by reaction with the THP-protected 6-(5-tributylstannyl-2-thienyl)-1-hexanol using modified Stille conditions inspired by the work of Fu and co-workers and Baldwin and co-workers.[38,39] Deprotection to give **T6-diol** and subsequent conversion to **T6-diacrylate** were accomplished using the same protocol as described for the **TPTTPT** and **TPEEPT** systems in Scheme 2.

All oligomers were characterized by ^{1}H and ^{13}C NMR spectroscopy and show narrow and well-defined signals as expected for monodisperse samples; identity and purity were confirmed by elemental analysis and high-resolution mass spectrometry (see Supporting Information for experimental procedures and full characterization of all new compounds).

Solution Properties

Electrochemistry. Cyclic voltammetry (CV) of oligomers and polymers tends to give broad peaks, which can obstruct an accurate characterization of the redox-active system investigated. In differential pulse voltammetry (DPV), on the other hand, the faradaic current is extracted and the redox processes can consequently be analyzed more precisely. We have studied the redox properties of **TPTTPT-Me$_2$**, **TPEEPT-Me$_2$**, and **T6-diol** in solution by both CV and DPV, and the results are presented in Figure 5 and Table 1.

The CV for **TPTTPT-Me$_2$** displays two well-resolved consecutive redox processes with half-wave potentials around 0.24 and 0.44 V (vs Fc/Fc^{+}).[40] Likewise, the voltammogram for **TPEEPT-Me$_2$** displays two fairly well-resolved consecutive redox processes with half-wave potentials around 0.15 and 0.50 V. The differential pulse voltammograms for **TPTTPT-Me$_2$** and **TPEEPT-Me$_2$** each reveal two well-defined and highly reversible anodic and cathodic processes with a high degree of symmetry; the half-wave potentials are now observed at slightly lower potentials than in the CV: 0.07 and 0.32 V for **TPTTPT-Me$_2$** and at −0.01 and 0.40 V for **TPEEPT-Me$_2$**. As expected, the first oxidation process occurs at a lower potential for **TPEEPT-Me$_2$** than for **TPTTPT-Me$_2$** because of the electron-donating ethylenedioxy substituents. The second oxidation process where the radical cation is converted to the dication occurs at a lower potential for **TPTTPT-Me$_2$** than for **TPEEPT-Me$_2$**. The same trend was observed for similar oligomeric systems by Roncali and co-workers and was ascribed to destabilization due to Coulombic repulsion between adjacent EDOT moieties in the dicationic state.[41] The values for **T6-**

(35) Turbiez, M.; Frere, P.; Roncali, J. *J. Org. Chem.* **2003**, *68*, 5357–5360.
(36) Turbiez, M.; Frere, P.; Allain, M.; Videlot, C.; Ackermann, J.; Roncali, J. *Chem.−Eur. J.* **2005**, *11*, 3742–3752.
(37) Deprotection of compounds **6** and **8** and subsequent oxidative coupling with ferric chloride afforded **TPTTPT-diol** and **TPEEPT-diol** in similar overall yields.
(38) Littke, A. F.; Schwarz, L.; Fu, G. C. *J. Am. Chem. Soc.* **2002**, *124*, 6343–6348.
(39) Mee, S. P. H.; Lee, V.; Baldwin, J. E. *Angew. Chem., Int. Ed.* **2004**, *43*, 1132–1136.
(40) In all of the CV experiments, a linear relationship between the oxidation current peak values and the square root of the scan rate was observed as expected for a diffusion-limited reaction at the electrode surface (see Supporting Information for voltammograms illustrating the scan rate dependence).
(41) Turbiez, M.; Frere, P.; Allain, M.; Videlot, C.; Ackermann, J.; Roncali, J. *Chem.−Eur. J.* **2005**, *11*, 3742–3752.

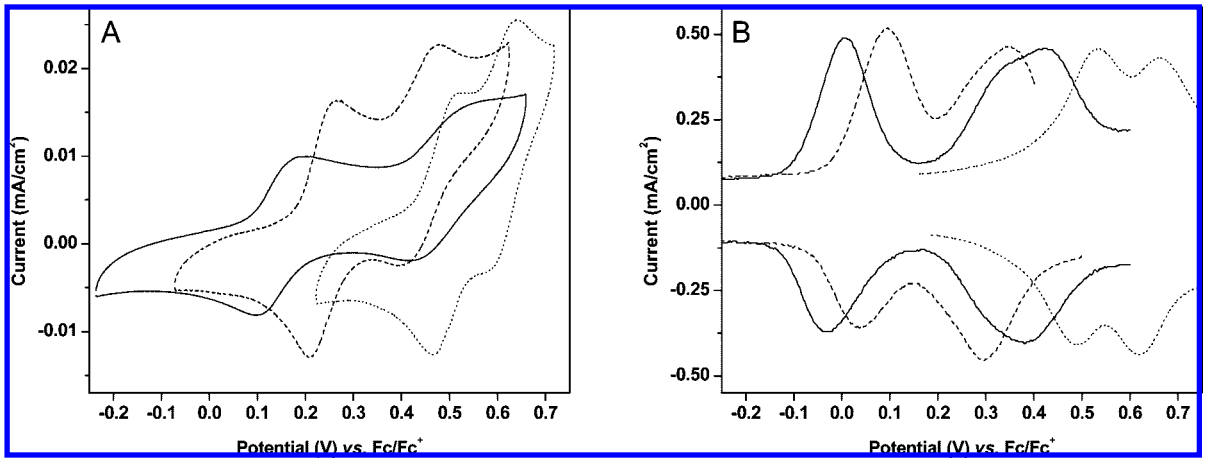

Figure 5. Cyclic voltammograms (A) and differential pulse voltammograms (B) of **TPTTPT-Me$_2$** (dashed lines), **TPEEPT-Me$_2$** (solid lines), and **T6-diol** (dotted lines) in dichloromethane. CV experiments performed with 0.1 mM oligomer and 0.1 M tetrabutylammonium perchlorate (scan rate 25 mV/s) and DPV with 1 mM oligomer and 0.1 M tetrabutylammonium hexafluorophosphate.

Table 1. Summarized Electrochemical Properties for the Oligomers in Solution[a]

	$E_{pa,1}$	$E_{pc,1}$	$E_{pa,2}$	$E_{pc,2}$
TPTTPT-Me$_2$[b]	0.27	0.21	0.48	0.39
TPTTPT-Me$_2$[c]	0.10	0.04	0.35	0.30
TPEEPT-Me$_2$[b]	0.20	0.10	0.57	0.42
TPEEPT-Me$_2$[c]	0.01	−0.03	0.42	0.38
T6-diol[b]	0.52	0.46	0.64	0.58
T6-diol[c]	0.53	0.49	0.66	0.62

[a] All potentials are reported in V vs ferrocene/ferrocenium. [b] CV data with 0.1 mM oligomer and 0.1 M tetrabutylammonium perchlorate in dichloromethane and scan rate 25 mV/s. [c] DPV data with 1 mM oligomer and 0.1 M tetrabutylammonium hexafluorophosphate in dichloromethane.

diol are in good agreement with earlier electrochemical studies of alkylated sexithiophenes under similar conditions.[42,43] In comparison with the sexithiophene oligomer, the **TPTTPT** and **TPEEPT** systems have lower half-wave potentials as one would expect when taking into account their electron-rich 2,5-dialkoxy-1,4-phenylene moieties.

Optical Spectroscopy. All of the oligomers show a strong absorption band in the violet-to-blue region of the visible spectrum due to the $\pi-\pi^*$ transition. A broad and featureless absorption band is observed for the **T6** (λ_{max} 423−425 nm; ε_{max} 45−49 000 M^{-1} cm^{-1}) and the **TPTTPT** oligomers (λ_{max} 430−432 nm; ε_{max} 55 000−67 000 M^{-1} cm^{-1}), whereas the **TPEEPT** system (λ_{max} 444−445 nm; ε_{max} 68 000−79 000 M^{-1} cm^{-1}) shows vibronic resolution attributed to the fact that the EDOT units induce a more coplanar structure due to favorable S−O interactions between neighboring phenylene and EDOT rings as was illustrated in the crystal structure of **PEEP** (Figure 4).

Chemical oxidation of **TPTTPT-Me$_2$** in dichloromethane with silver triflate affords a new transition with two peaks at 665 and 733 nm as well as a broad transition in the infrared (∼1630 nm) while the $\pi-\pi^*$ transition of the neutral state gradually disappears (Figure 6A). Investigation of the temperature dependence in this oxidized state (Figure 6B) reveals that the radical cation coexists with the π-dimer below room temperature;[44–47] lowering of the temperature shifts the equilibrium from the radical cation (733, 1630 nm) toward the dimeric species (665, 1187 nm). Upon further oxidation with nitrosonium hexafluorophosphate, the absorption bands associated with the radical cation and the π-dimer species disappear and a new transition from the dication (1188, 1029 nm) is observed (Figure 6C). As also depicted in Figure 6 (inserted photographs), the neutral solution of **TPTTPT-Me$_2$** is yellow, the radical cation is blue, and the dication is quite transparent and color neutral since it mostly absorbs outside the visible region.

Solution oxidation of **TPEEPT-Me$_2$** (Figure 7 and Table 2) gives results very similar to what was described for **TPTTPT-Me$_2$** above. Additionally, the solution oxidation of **T6-diol** was examined (absorption spectra included in Supporting Information), and in agreement with previous optical studies of sexithiophenes,[48,49] absorption bands were assigned to the neutral state (424 nm), the radical cation (806, 1557 nm), the π-dimer (702, 1124 nm), and the dication (893, 1003 nm). Compared to that of 3′,3′′′′-didodecylsexithiophene, which has unsubstituted α-positions, the absorption bands of **T6-diol** are red-shifted 20−50 meV (neutral and π-dimer species) to 60−80 meV (radical cation and dication species).

While the neutral species and the dications of the oligomers show one HOMO−LUMO transition, the radical cations show two transitions, one corresponding to a HOMO−SOMO transition (low-energy transition) and one corresponding to a SOMO−LUMO transition (high-energy transition), as illustrated schematically in Figure 8.

The electron-pairing energy stabilizes both the neutral and the dication ground states (but not the radical cation ground state), which explains why the absorption bands of the neutral species and the dication are observed at shorter wavelengths

(42) Roncali, J.; Giffard, M.; Jubault, M.; Gorgues, A. *J. Electroanal. Chem.* **1993**, *361*, 185–191.
(43) Nessakh, B.; Horowitz, G.; Garnier, F.; Deloffre, F.; Srivastava, P.; Yassar, A. *J. Electroanal. Chem.* **1995**, *399*, 97–103.
(44) Bauerle, P.; Segelbacher, U.; Maier, A.; Mehring, M. *J. Am. Chem. Soc.* **1993**, *115*, 10217–10223.
(45) Hill, M. G.; Penneau, J. F.; Zinger, B.; Mann, K. R.; Miller, L. L. *Chem. Mater.* **1992**, *4*, 1106–1113.
(46) Tabakovic, I.; Maki, T.; Miller, L. L.; Yu, Y. A. *Chem. Commun.* **1996**, 1911–1912.
(47) Hill, M. G.; Mann, K. R.; Miller, L. L.; Penneau, J. F. *J. Am. Chem. Soc.* **1992**, *114*, 2728–2730.
(48) Bauerle, P.; Segelbacher, U.; Gaudl, K. U.; Huttenlocher, D.; Mehring, M. *Angew. Chem., Int. Ed.* **1993**, *32*, 76–78.
(49) Fichou, D.; Horowitz, G.; Xu, B.; Garnier, F. *Synth. Met.* **1990**, *39*, 243–259.

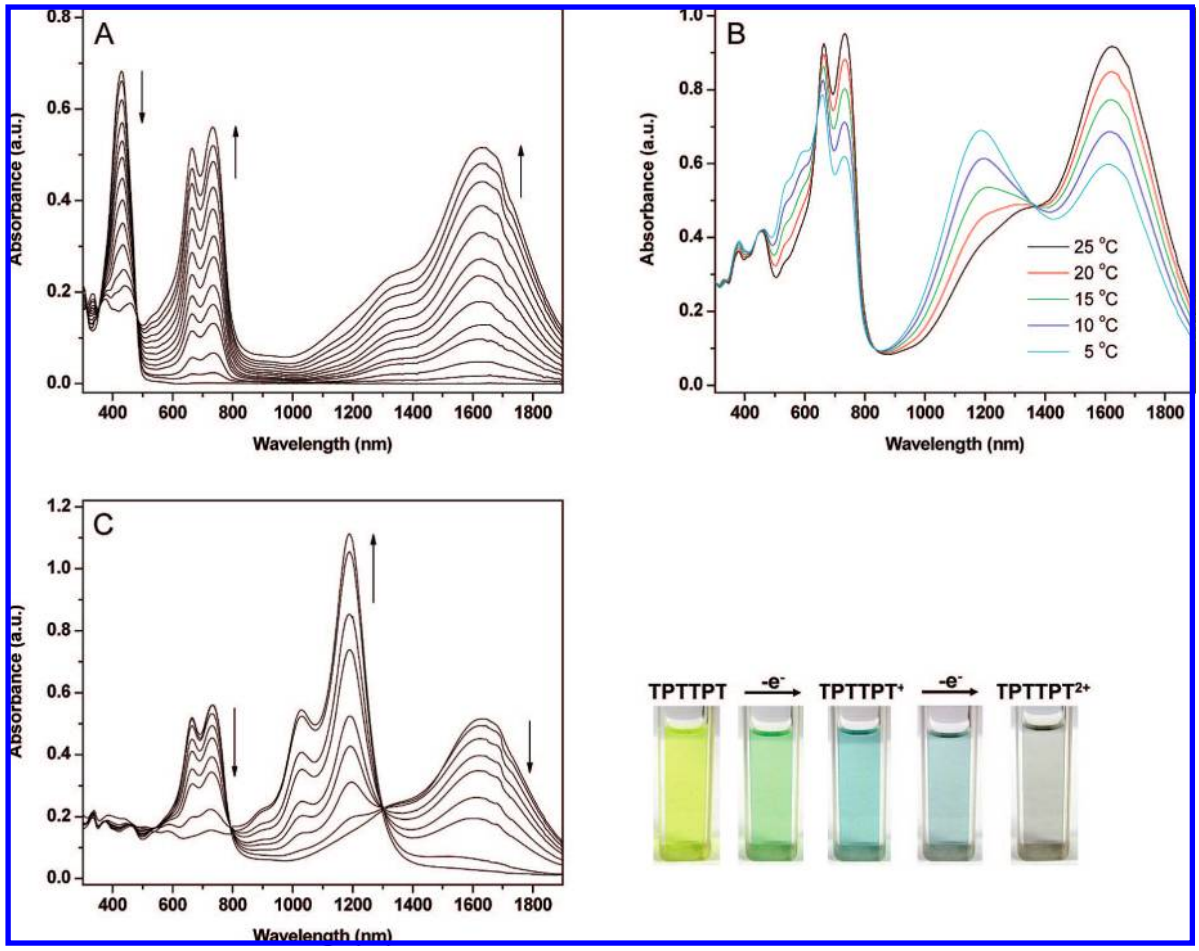

Figure 6. Solution oxidation of **TPTTPT-Me$_2$** in dichloromethane. (A) Conversion from neutral to radical cation and π-dimer species, (B) temperature dependence of the monomer/dimer equilibrium, (C) conversion from radical cation to dication, and photographs of the observed color changes.

than the high- and low-energy transitions of the radical cation, respectively. The two transitions from the π-dimer are blue-shifted (0.17−0.23 eV for the high-energy transition and 0.19−0.30 eV for the low-energy transition) compared to the monomeric radical cation; this is indicative of a face-to-face interaction and is normally referred to as a Davydov blue-shift.[44] The absorption bands from the radical cation and the π-dimer overlap significantly for all three oligomers, which makes it complicated to determine the dimer formation enthalpy. Qualitatively, the dimer formation enthalpy is found to be largest for the **TPTTPT** system and smallest for the **TPEEPT** system. This is most likely governed by the degree of charge delocalization; the radical cation of **TPEEPT** has a more localized charge distribution than **TPTTPT** and **T6** and will therefore, because of charge repulsion, be less prone to form a π-dimer. For the dications, we observe vibronic fine structure in all three cases, a phenomenon caused by a more quinoidal structure and hence increased planarity in the oxidized systems. We furthermore note that these vibronic splittings fall in the range ΔE = 0.15−0.17 eV, which is in good agreement with previous studies of other oligomeric thiophene systems.[44,45,50]

Electron Paramagnetic Resonance Spectroscopy. Electron paramagnetic resonance (EPR) spectroscopy of **TPTTPT-Me$_2$** and **TPEEPT-Me$_2$** in dichloromethane confirmed the presence of the paramagnetic radical cation upon oxidation (the π-dimer is EPR silent) and the subsequent conversion to the EPR silent dication upon further oxidation (Figures 9 and 10). The radical cation of **TPTTPT-Me$_2$** has an EPR signal centered at a g value of 2.012 with a peak-to-peak width of 5.3 G, while the signal from radical cation of **TPEEPT-Me$_2$** is centered at g = 2.008 with ΔH_{pp} = 4.2 G; these EPR characteristics compare well to earlier studies of oligothiophenes by Tour and co-workers.[50] No hyperfine coupling was observed for either of the two systems, a finding that could be attributed to the delocalization of the radical cation wave function, which results in sampling a large number of different isotropic interactions with neighboring hydrogens. While hyperfine coupling has been observed for short oligothiophenes,[46,47] longer π-conjugated oligomers generally give rise to broad and featureless EPR signals.[51,52] The slightly broader line width observed for the **TPTTPT** system than that for the **TPEEPT** system is most likely due to the larger number of hydrogens attached directly to the aromatic core of **TPTTPT-Me$_2$** (12 vs eight hydrogen atoms). Incomplete conversion from the radical cation to the dication explains the small EPR signals observed for the dication preparation of both **TPTTPT-Me$_2$** and **TPEEPT-Me$_2$** (Figure 10, dotted lines).

Solid-State Properties

Electrochemistry. To investigate the redox properties of the oligomers in the solid state, we focused on thin films of the

(50) Guay, J.; Kasai, P.; Diaz, A.; Wu, R. L.; Tour, J. M.; Dao, L. H. *Chem. Mater.* **1992**, *4*, 1097–1105.
(51) Janssen, R. A. J.; Moses, D.; Sariciftci, N. S. *J. Chem. Phys.* **1994**, *101*, 9519–9527.
(52) Kanemoto, K.; Kato, T.; Aso, Y.; Otsubo, T. *Phys. Rev. B* **2003**, *68*, 092302.

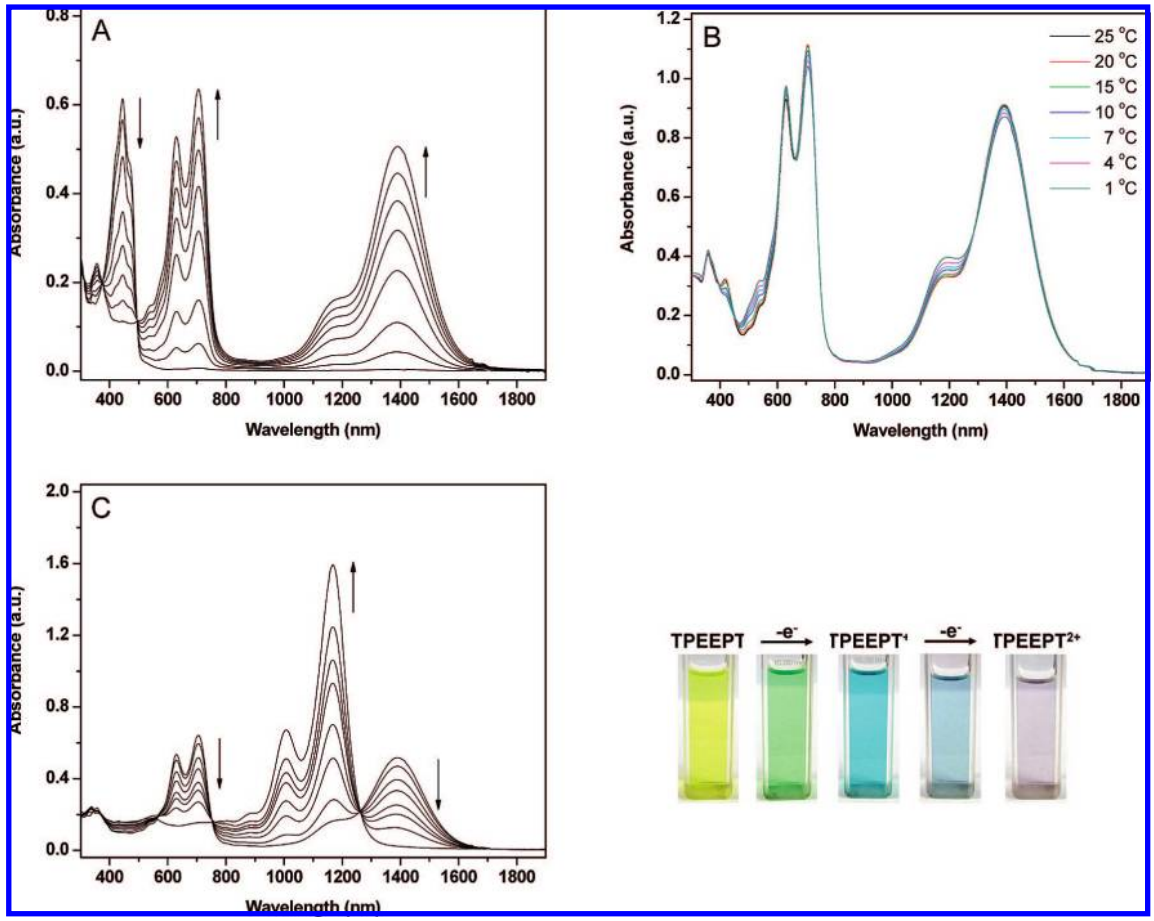

Figure 7. Solution oxidation of **TPEEPT-Me$_2$** in dichloromethane. (A) Gradual conversion from neutral to radical cation and π-dimer species, (B) temperature dependence of the monomer/dimer equilibrium, (C) conversion from radical cation to dication, and photographs of the observed color changes.

Table 2. Absorption Maxima (nm) for the Neutral (M), Radical Cation ($M^{+\cdot}$), π-Dimer (M_2^{2+}), and Dication (M^{2+}) of **TPTTPT-Me$_2$**, **TPEEPT-Me$_2$**, and **T6-Diol** in Dichloromethane Solution (10^{-5} M).

	TPTTPT-Me$_2$	TPEEPT-Me$_2$	T6-diol
M	430	445	424
$M^{\bullet+}$	733, 1630	705, 1389	806, 1557
M_2^{2+}	665, 1187	630, 1198	702, 1124
M^{2+}	1029, 1188	1007, 1167	893, 1003

diacrylate oligomers; upon UV irradiation of these films, the diacrylates polymerize to form cross-linked networks, which renders them insoluble in all common organic solvents and hence suitable for solid-state electrochemistry.

Redox properties of the cross-linked films in acetonitrile-supported electrolyte are depicted in Figure 10, and the results are summarized in Table 3. For **TPEEPT-diacrylate**, the two consecutive redox processes are well-resolved, whereas two poorly resolved peaks (**TPTTPT-diacrylate**) or one broad peak with shoulder features (**T6-diacrylate**) are observed for the other two systems. Some electrochemical irreversibility is expressed through the lower current passed during the cathodic sweep as compared to the current passed during the anodic sweep. Hysteresis effects are observed for all three systems, and potential differences as large as 450 mV between the oxidation and the reduction peaks are seen for **T6-diacrylate**.

From the onset of oxidation, it is estimated that **T6-diacrylate** has a HOMO value of 5.4 eV; changing the two 3-alkylthiophenes into two 2,5-dialkoxy-1,4-phenylenes does not affect the HOMO value as it is found to be 5.4−5.5 eV for **TPTTPT-diacrylate** also. Subsequent conversion of the two inner thiophenes into the more electron-rich EDOTs raises the HOMO value to approximately 5.2 eV as observed for **TPEEPT-diacrylate**.

Numerous studies have illustrated that dioxythiophene-containing systems have a significantly increased stability of the oxidized states as compared to unsubstituted thiophene and alkylthiophene systems.[53–57] This observation is also made in this study when comparing the redox processes of **TPTTPT-diacrylate**, **TPEEPT-diacrylate**, and **T6-diacrylate** and is particularly pronounced when investigating the solid-state electrochemistry in a dichloromethane-supported electrolyte. While **TPTTPT-diacrylate** and **T6-diacrylate** films in dichloromethane show limited current responses upon electrochemical oxidation and continuously lose electroactivity, incorporation of EDOT moieties greatly enhances the redox stability. This is illustrated for **TPEEPT-diacrylate** in Figure 11; both the CV and the DPV experiments reveal two well-separated oxidation peaks followed by two reduction peaks offering a high degree of symmetry and thus a high degree of chemical reversibility. The first half-wave potential is observed at 0.05 V in both CV

(53) Jonas, F.; Heywang, G. *Electrochim. Acta* **1994**, *39*, 1345–1347.
(54) Yamato, H.; Ohwa, M.; Wernet, W. *J. Electroanal. Chem.* **1995**, *397*, 163–170.
(55) Pei, Q.; Zuccarello, G.; Ahlskog, M.; Inganas, O. *Polymer* **1994**, *35*, 1347–1351.
(56) Dietrich, M.; Heinze, J.; Heywang, G.; Jonas, F. *J. Electroanal. Chem.* **1994**, *369*, 87–92.
(57) Heywang, G.; Jonas, F. *Adv. Mater.* **1992**, *4*, 116–118.

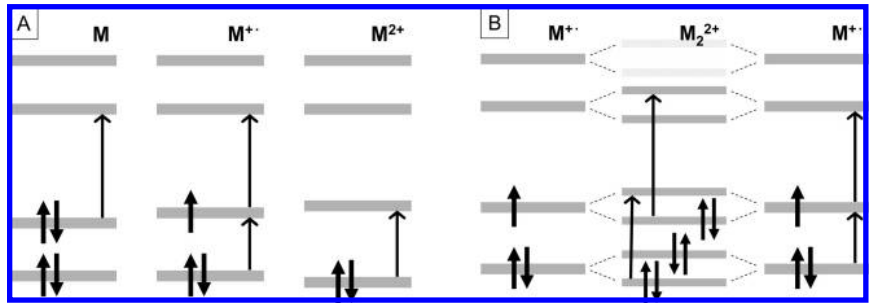

Figure 8. (A) Frontier molecular orbitals and dipole-allowed transitions for a neutral species (M), a radical cation ($M^{\bullet+}$), and a dication (M^{2+}). (B) Frontier orbitals and allowed transitions for the π-dimer based on linear combination of molecular orbitals for the radical cation.

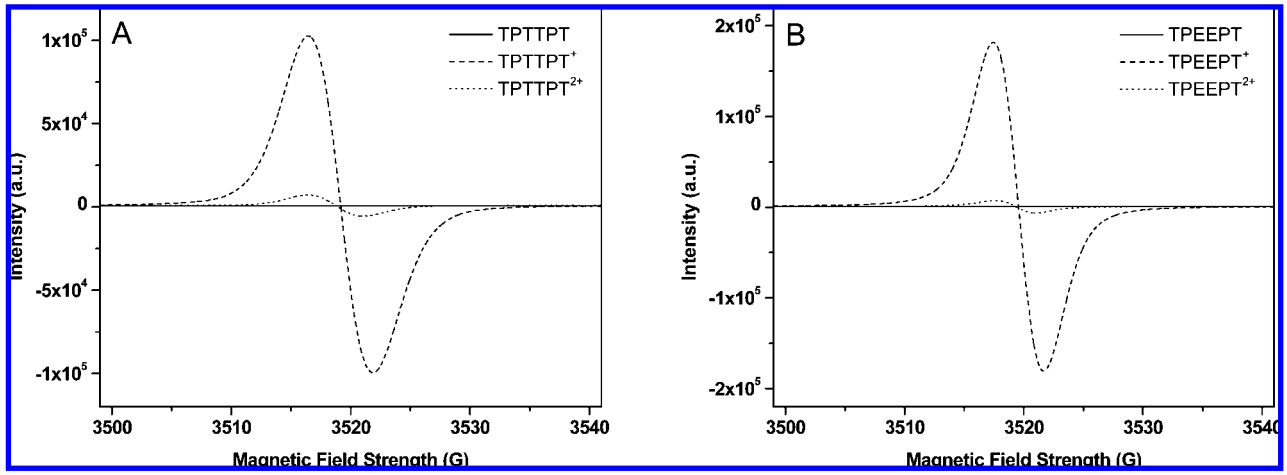

Figure 9. EPR spectra of the neutral (solid line), radical cation (dashed line), and dication (dotted line) of (A) **TPTTPT-Me$_2$** and (B) **TPEEPT-Me$_2$** in dichloromethane (1 mM).

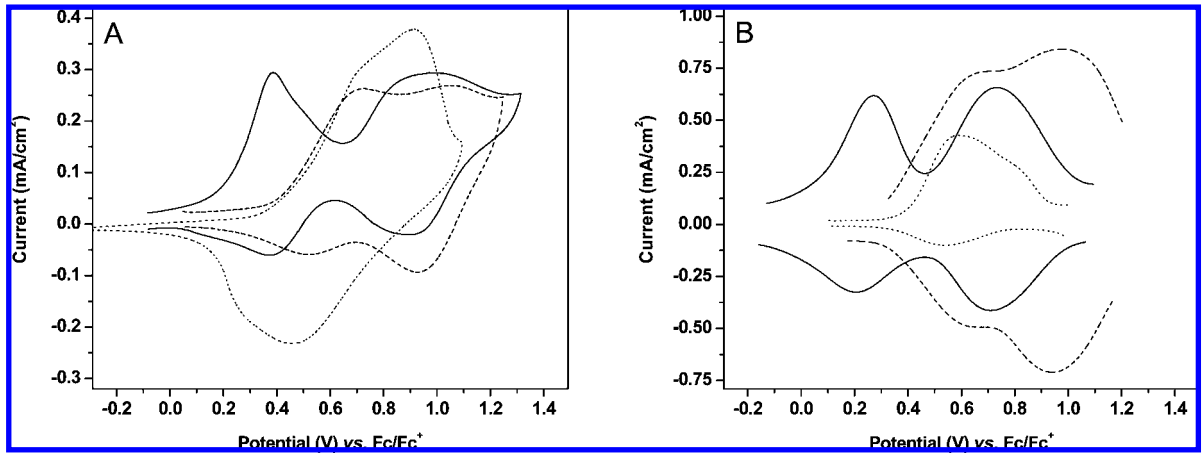

Figure 10. Cyclic voltammograms (A) and differential pulse voltammograms (B) of cross-linked films of **TPTTPT-diacrylate** (dashed lines), **TPEEPT-diacrylate** (solid lines), and **T6-diacrylate** (dotted lines) on ITO-coated glass in 0.1 M tetrabutylammonium perchlorate in acetonitrile (CV scan rate 150 mV/s).

and DPV (Table 3), while the second half-wave potential is identified at 0.64 V (CV) and 0.56 V (DPV).[40] These potentials are significantly lower than the values obtained in acetonitrile-supported electrolyte but compare well with the solution data for **TPEEPT-Me$_2$** also obtained in dichloromethane. From the onset of oxidation, the HOMO energy level for **TPEEPT-diacrylate** is estimated to be approximately 5.0 eV under these conditions.

The electrochemical results presented here on the three oligomer systems in the solid state clearly show that cross-linked films of **TPEEPT-diacrylate** are the most electrochemically stable materials of the three. Films of **TPTTPT-diacrylate** and **T6-diacrylate** show poor electrochemical stability in both acetonitrile and dichloromethane. Films of **TPEEPT-diacrylate**, on the other hand, switch nicely, especially in a dichloromethane-supported electrolyte, between a yellow neutral state, a blue radical cation state, and a more transparent blue/purple dication state. Thus, compared to that of **TPTTPT** and **T6**, the **TPEEPT** chromophore proves to be a far more promising candidate for electrochromic applications, and the diacrylate functionality offers a convenient means of controlling solubility.

Table 3. Summarized Electrochemical Properties for the Diacrylate Oligomers in the Solid State[a]

	E_{onset}	$E_{pa,1}$	$E_{pc,1}$	$E_{pa,2}$	$E_{pc,2}$
TPTTPT[b]	0.41	0.72	0.52	1.05	0.93
TPTTPT[c]	0.33	0.68	0.62	0.98	0.94
TPEEPT[b]	0.20	0.39	0.37	0.99	0.89
TPEEPT[c]	0.06	0.27	0.20	0.73	0.71
T6[b]	0.33	0.70	0.25	0.91	0.46
T6[c]	0.35	0.58	0.53		
TPEEPT[d]	−0.06	0.07	0.03	0.66	0.61
TPEEPT[e]	−0.13	0.10	0.00	0.61	0.50

[a] All potentials are reported in V vs ferrocene/ferrocenium. All experiments were performed with cross-linked films on ITO-coated glass with 0.1 M tetrabutylammonium perchlorate as electrolyte. [b] CV data in acetonitrile and scan rate 150 mV/s. [c] DPV data in acetonitrile. [d] CV data in dichloromethane and scan rate 25 mV/s. [e] DPV data in dichloromethane.

Optical Spectroscopy. Thin film absorption spectra (Figure 12, Table 4) indicate the expected more coplanar structure in the solid state compared to solution for all three systems, although indications of a less ordered packing are observed for **TPEEPT-diacrylate**. Figure 12 additionally pictures the changes in the optical properties when cross-linking the spray-cast films. The cross-linking process is associated with a small blue-shift (7−11 nm) for **TPTTPT-diacrylate** and **T6-diacrylate**, which indicates that these two systems rearrange to slightly less coplanar conformations upon the photopolymerization. **TPEEPT-diacrylate**, on the other hand, adapts a more coplanar structure overall during the cross-linking process as judged from the increased intensity of the low-energy peaks and decreased intensity of the high-energy peaks. For all three systems, loss of order during the UV irradiation is indicated by the loss of vibronic coupling in the absorption spectra. It is conceivable that the cross-linking process is associated with molecular rearrangements that would lead to an overall loss of order in the film.[32] The optical band gaps, as determined from the low-energy band-edges, fall in the range 2.3−2.4 eV.

Spectroelectrochemistry. To further demonstrate the high stability of the **TPEEPT** system in its oxidized states, spectroelectrochemistry was carried out for a spray-cast and subsequently cross-linked film of **TPEEPT-diacrylate** as depicted in Figure 13. At −0.24 V (vs Fc/Fc^+), the film is neutral and therefore displays only the $\pi-\pi^*$ transition at 452 nm. As the potential is increased stepwise to 0.34 V, the absorption band from the neutral film disappears gradually, while two broad bands ascribed to the radical cation (monomeric and/or dimeric) emerge at 603 and 1180 nm; the latter blue-shifts gradually to 1140 nm as it increases in intensity (Figure 13A). Further increment of the potential to 0.86 V is accompanied by the gradual appearance of a transition from the dication (1000 nm) at the expense of the absorption bands from the radical cation as illustrated in Figure 13B. Visualization of the optical changes is aided by observation of the difference spectra obtained by subtraction of the first spectrum in a series from the following spectra as illustrated in Figure 13C,D. Especially for the conversion from radical cation to dication, the regular absorption spectra are complicated by the overlap of the radical cation and dication absorption bands, but this is overcome by examination of the difference spectra instead. This deconvolution reveals the gradual disappearance of the two bands from the radical cation and the corresponding appearance of the dication absorption band. It is furthermore revealed by this approach that a low-intensity absorption band around 685 nm is associated with the dication absorption band at 1000 nm. The inserted photographs show the distinct color changes from a bright yellow neutral film to a clear blue (radical cation), and subsequently on to an almost transparent dicationic state with a residual bluish component from the radical cation and a slight purple color from the 685-nm band. Comparison with the solution oxidation data (Figure 7) reveals that the positions of the various absorption bands are more or less unchanged during the transition from solution to the solid state. However, the bands in the solid state are broadened and lack the resolution observed in solution, most likely due to the rigidification of the films taking place during cross-linking, which locks the conformation and hinders any substantial reorganization in the film during the oxidation processes.

Photopatterning and Switching Studies. After having established the chemical stability of the **TPEEPT** system in its various oxidized states, the high degree of redox reversibility, and excellent multicolored electrochromic behavior, the next step was to employ the diacrylate functionality of **TPEEPT-diacrylate** for photopatterning purposes. Thin films of **TPEEPT-diacrylate** cross-link successfully within a few hours with no sign of degradation of the **TPEEPT** chromophores. Figure 14 shows how the absorption increases and the emission decreases when the films are thermally annealed and subsequently photopolymerized, a finding that indicates that the degree of structural order is increasing during the process.[58]

As illustrated in Figure 15, this strategy (in combination with simple mask fabrication) can be applied in a straightforward photopatterning process to create defect-free patterns with at least submillimeter resolution. Photopatterned films of **TPEEPT-diacrylate** show the same optical, electrochemical, and spectroelectrochemical characteristics as already discussed for homogeneous films of **TPEEPT-diacrylate**; the capability of manifesting three distinct colors when going from neutral to radical cation and to dication is also conserved as obvious from Figure 15B−D.

To further probe the electrochromic properties of the cross-linked **TPEEPT-diacrylate** material, the switching characteristics for several films were investigated by monitoring the transmittance at the wavelength of maximum contrast during repeated redox stepping experiments (Table 5). Figure 16 shows the chronoabsorptometry at a wavelength of 600 nm for the electrochromic switching between the neutral state (yellow, λ_{max} 452 nm) and the radical cation (blue, λ_{max} 603 nm) with 30-s delays between each redox switch. For a relatively thick film (225 nm, Figure 16A), the percent transmittance is 89.2% in the bleached state (yellow) and 26.7% in the colored state (blue), which gives a contrast value of 62.5% ($\Delta\%T$). For a thinner film (85 nm, Figure 16B), the percent transmittances are 99.3% (bleached) and 61.5% (colored), resulting in a contrast ratio of 37.8%; after 400 switches (7 h) of the thinner film, the contrast ratio decayed to approximately 30%. A good correlation was observed between film thickness and contrast ratio as obvious from the data in Table 5 (see Supporting Information for the complete set of switching data). Response times for achieving the blue state (600 nm coloration, t_c) and the yellow state (600 nm bleaching, t_b) were determined as the time it took to reach 95% of the ultimate change in $\%T$.[59] As expected, the switching times were highly dependent on film thickness: for the thinner films, response times of 2.3−2.4 s for coloration and ap-

(58) Kim, Y.; Cook, S.; Tuladhar, S. M.; Choulis, S. A.; Nelson, J.; Durrant, J. R.; Bradley, D. D. C.; Giles, M.; McCulloch, I.; Ha, C. S.; Ree, M. *Nat. Mater.* **2006**, *5*, 197–203.

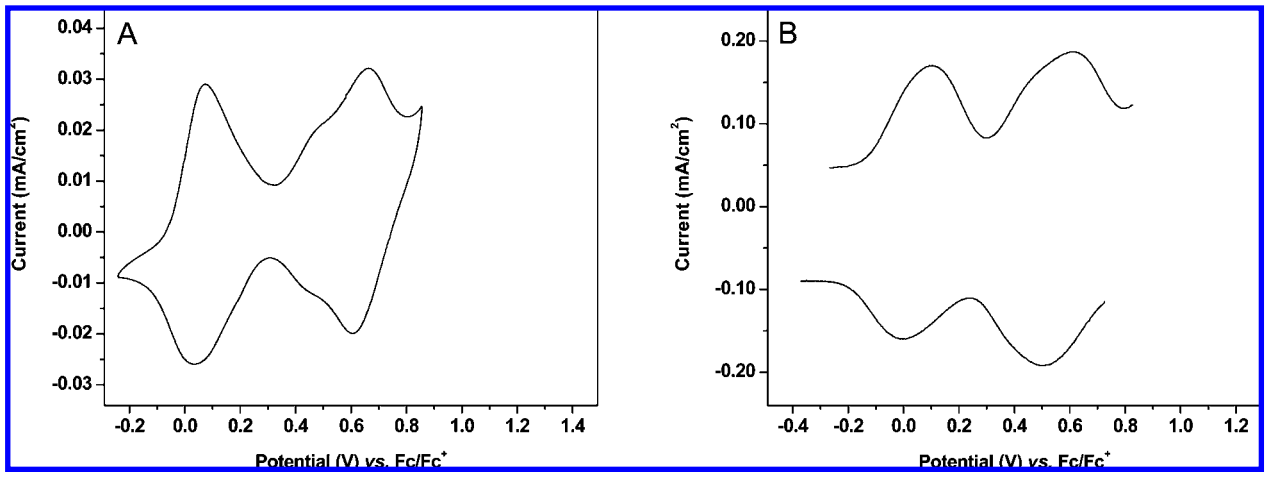

Figure 11. Cyclic voltammograms (A) and differential pulse voltammograms (B) of cross-linked films of **TPEEPT-diacrylate** on ITO-coated glass in 0.1 M tetrabutylammonium perchlorate in dichloromethane (CV scan rate 25 mV/s).

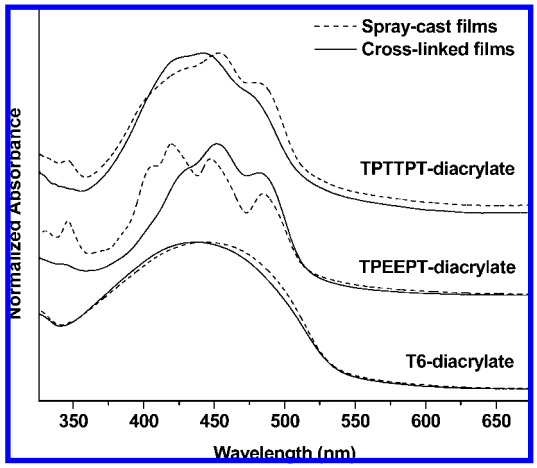

Figure 12. Normalized absorption spectra of films of **TPTTPT-diacrylate** (top), **TPEEPT-diacrylate** (middle), and **T6-diacrylate** (bottom) spray-cast from toluene/dichloromethane (9:1) before (dashed lines) and after (solid lines) cross-linking.

Table 4. Summarized Optical Properties for the Oligomers

	λ_{max} (nm)[a]	λ_{max} (nm)[b]	λ_{max} (nm)[c]	E_{onset} (eV)[c]
TPTTPT-diacrylate	432	454, 480	443	2.4
TPEEPT-diacrylate	445	420, 447, 485	452, 482	2.4
T6-diacrylate	425	444	437	2.3

[a] In THF solution. [b] Films spray-cast from toluene/dichloromethane. [c] Cross-linked films.

proximately 10 s for bleaching were observed, while the thicker films showed coloration times of 3.6 s (115 nm film) and 4.6 s (225 nm film) and bleaching times of 14.5 s (115 nm) and 21.1 s (225 nm). Apart from the slow bleaching process, these switching and contrast characteristics are comparable to other EDOT-containing electrochromic materials described in the literature,[60] but it should be noted that other electrochromic π-conjugated polymers with much faster switching times (100−300 ms) and enhanced lifetimes have been reported.[25,61]

The instability observed during prolonged switching is primarily caused by an incomplete return to the neutral state (Figure 16B) and seems to be connected with the relatively long switching time observed for the bleaching process, which is approximately four times slower than the coloration process. The cross-linking process is likely to cause a tighter organization with more closely packed chains. Therefore, the coloration process, which takes the oligomer from its neutral to its oxidized form, should take place easily since it is associated with a planarization of the oligomer backbone as the quinoidal radical cation forms. On the other hand, the bleaching process is associated with the conversion from the quinoidal oxidized species to the slightly less planar neutral form and could therefore be hindered by the tight locked packing in the cross-linked network. Further indication of the tight packing is also seen with the significantly increased switching times with increased film thickness.

Conclusions

We presented two novel chromophores (**TPTTPT** and **TPEEPT**), which were synthesized both as methyl-terminated model compounds and telechelic analogues together with two novel telechelic sexithiophene derivatives (**T6-diol** and **T6-diacrylate**). Structural characterization based on single crystal structures of **PTTP** and **PEEP** indicates that a central biEDOT unit (due to attractive intramolecular sulfur−oxygen interactions) causes a higher degree of molecular planarity than a bithiophene unit. Comparison with the crystal structure of 3,3‴-didocylquaterthiophene[62] suggests a close resemblance between the **PEEP** motif and the dialkylated quaterthiophene, while **PTTP** is somewhat less planar. The overall structural rigidifying effect of the EDOTs is confirmed by the vibronic resolution observed in the optical absorption spectra for **TPEEPT**, but not for **TPTTPT** or **T6**.

In dichloromethane, we found the oxidized species of all three oligomeric systems to be quite stable, which allowed for a thorough characterization of the redox properties and the different oxidized species involved. The all-thiophene **T6** system has the highest first oxidation potential; introduction of the more

(59) Gaupp, C. L.; Welsh, D. M.; Rauh, R. D.; Reynolds, J. R. *Chem. Mater.* **2002**, *14*, 3964–3970.
(60) Kumar, A.; Welsh, D. M.; Morvant, M. C.; Piroux, F.; Abboud, K. A.; Reynolds, J. R. *Chem. Mater.* **1998**, *10*, 896–902.
(61) Lu, W.; Fadeev, A. G.; Qi, B. H.; Smela, E.; Mattes, B. R.; Ding, J.; Spinks, G. M.; Mazurkiewicz, J.; Zhou, D. Z.; Wallace, G. G.; MacFarlane, D. R.; Forsyth, S. A.; Forsyth, M. *Science* **2002**, *297*, 983–987.
(62) Azumi, R.; Gotz, G.; Debaerdemaeker, T.; Bauerle, P. *Chem.−Eur. J.* **2000**, *6*, 735–744.

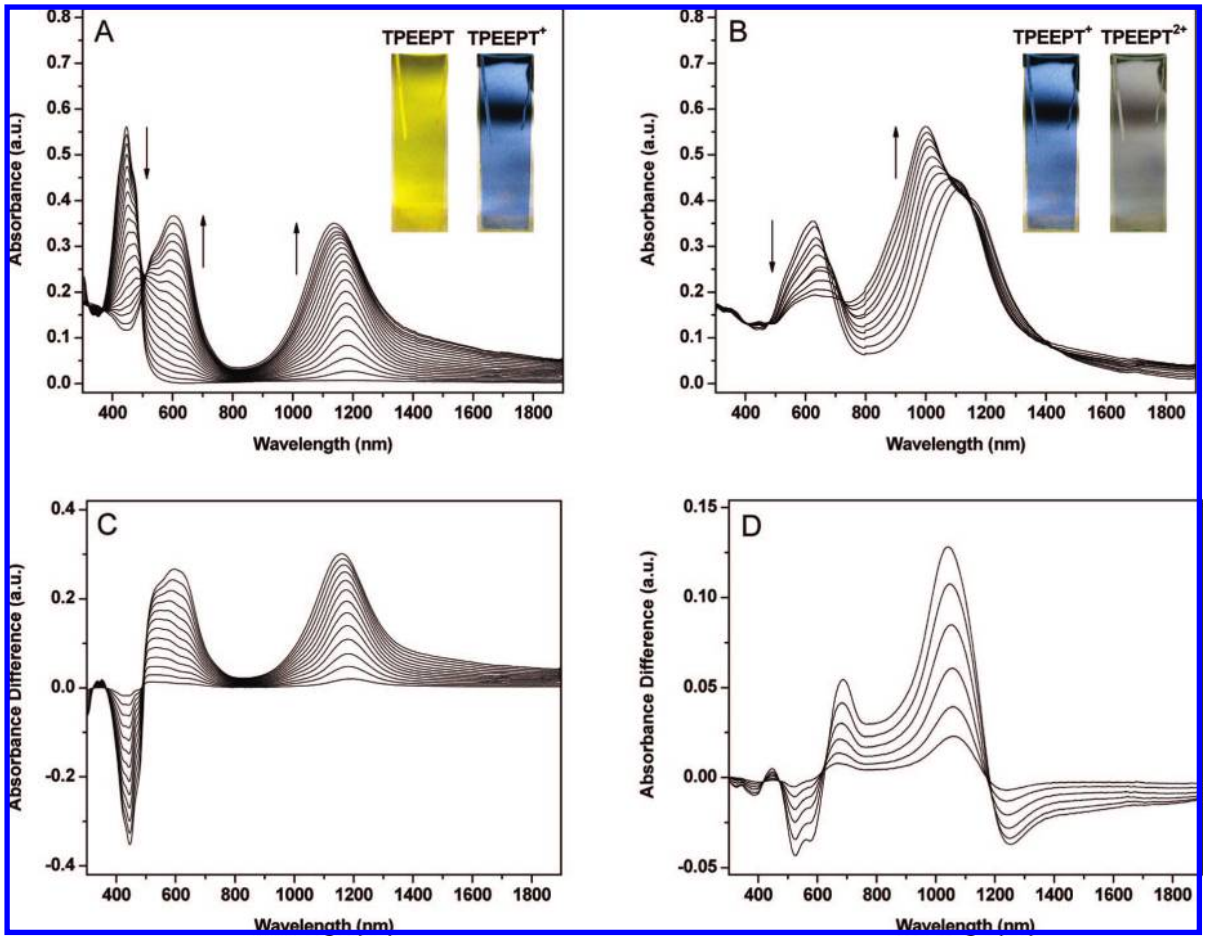

Figure 13. Spectroelectrochemistry for a cross-linked film of **TPTTPT-diacrylate** on ITO-coated glass in 0.1 M tetrabutylammonium perchlorate in dichloromethane. (A) Gradual conversion from neutral to radical cation species (potential stepped from −0.24 to 0.34 V vs Fc/Fc^{+}), (B) conversion from radical cation to dication (potential stepped from 0.34 to 0.86 V vs Fc/Fc^{+}), (C) difference absorption spectra showing the optical changes during the conversion from neutral to radical cation, and (D) difference absorption spectra for the conversion from radical cation to dication.

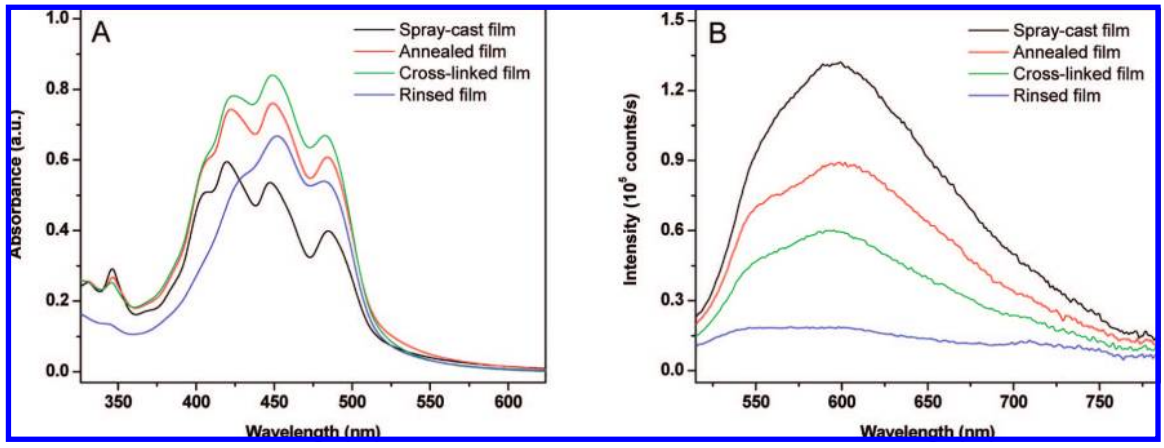

Figure 14. UV−vis (A) and fluorescence (B) spectra of a thin film of **TPEEPT-diacrylate**. Film was spray-cast and then annealed (60 °C in vacuum overnight) before being cross-linked (UV-curing for 10 min) and then rinsed with tetrahydrofuran.

electron-rich dialkoxybenzene unit lowers the oxidation potential (**TPTTPT**), and a further decrease is seen when introducing the EDOT unit. Although **TPEEPT** thus has the most stable radical cation, the next one-electron oxidation occurs more easily for **T6** ($\Delta E = 120-130$ mV) and for **TPTTPT** ($\Delta E = 200-250$ mV) than for **TPEEPT** ($\Delta E = 350-410$ mV) because of charge repulsion in the dication of **TPEEPT** due to a lower degree of charge delocalization along the backbone. These electrochemical properties are reflected very well by the optical properties of the oxidized species. The red-shift associated with the first oxidation (from neutral to radical cation) is small for **TPEEPT** (1.03 eV), somewhat larger for **TPTTPT** (1.19 eV), and even larger for **T6** (1.38 eV). For the second oxidation (from radical cation to dication), on the other hand, the trend is opposite with the red-shift being only 0.30 eV for **T6**, 0.65 eV for **TPTTPT**, and 0.70 eV for **TPEEPT**. Each of the radical cations is in

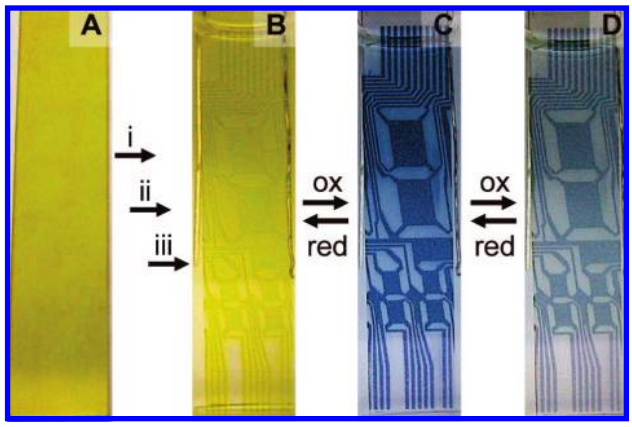

Figure 15. Photopatterning process for a spray-cast film of **TPEEPT-diacrylate** (A). After (i) applying a mask, (ii) irradiating with UV light, and (iii) washing with tetrahydrofuran, we found that the cross-linked and patterned film appears as illustrated in (B). Subsequent electrochemical oxidation affords the blue radical cation (C) and the pale blue/transparent dication (D).

Table 5. Summarized Switching Properties for Four Cross-Linked **TPEEPT-Diacrylate** Films of Various Thicknesses

film thickness (nm)	Δ%*T*	t_c (s)	t_b (s)
80	34.4	2.4	10.4
85	37.8	2.3	9.6
115	45.4	3.6	14.5
225	62.5	4.6	21.1

[a] All experiments were performed with cross-linked films on ITO-coated glass with 0.1 M tetrabutylammonium perchlorate as electrolyte. Switching was monitored as the percent transmittance (%*T*) at 600 nm with a 30-s delay for each potential (−0.65 and 0.25 V), and switching times were determined as the time it took to reach 95% of the ultimate change in %*T*.

equilibrium with its corresponding π-dimer in solution; again, we see evidence for the fact that the EDOTs tend to favor a more localized charge distribution since **TPEEPT** is less prone to dimerization than **TPTTPT** and **T6**.

The herein reported oligomers are all highly soluble in many common organic solvents and can thus easily be spin- or spray-cast onto various substrates to form thin homogeneous films. Furthermore, by the attachment of acrylate functionalities to the oligomers, we were able to convert the solution-processed films into insoluble cross-linked networks by UV curing. Thus, we can take advantage of the very convenient solution processibility as well as subsequent solid-state processing, which "locks" the film into an insoluble solid state. In general, we found the oligomers to behave very similarly in the solid state to what was observed in solution. The cross-linked film of **TPEEPT-diacrylate** has the lowest first oxidation potential, but opposite to what was observed in solution, **T6** ($E_{1/2}$ = 0.47 V) is now more easily oxidized to the radical cation than **TPTTPT** ($E_{1/2}$ = 0.62 V), which is probably caused by a more coplanar organization for **T6** in the solid state than for **TPTTPT** as also indicated in the single crystal structures. Again, we observe the next one-electron oxidation to the dication to occur more easily for **T6** (ΔE = 210 mV) and for **TPTTPT** (ΔE = 310−370 mV) than for **TPEEPT** (ΔE = 460−480 mV).

In particular, we discovered that a cross-linked film of **TPEEPT-diacrylate** is quite stable in its different oxidized states and thus undergoes two consecutive and very reversible redox processes even under ambient conditions. Further characterization by spectroelectrochemistry reveals two distinct color changes when going from the bright yellow neutral material to the clear blue radical cation and subsequently to the dication, which is transparent with a small residual gray color. The promising electrochromic properties of this material are further verified by our initial switching studies showing good contrast ratios and reasonable coloration and bleaching times during at least 400 cycles. To utilize the cross-linkable acrylate functionality to its fullest, we have (as a proof of concept) shown how a **TPEEPT-diacrylate** film successfully can be subjected to a simple photopatterning process.

To summarize, we developed a series of telechelic oligomers with various π-conjugated cores. From our studies, it is obvious that 3,4-dioxythiophene moieties (here in the form of EDOT units) offer an enhanced stability of the oxidized states, which makes these oligomers superior for electrochromic devices as compared to the thiophene- and phenylene-based systems. Further synthetic efforts including modifications of the 3,4-dioxythiophene (incorporation of ProDOT, dialkyl-ProDOT, etc.), the relative positions of the 3,4-dioxythiophene units in the oligomer, and variations in the length of the oligomer and the attractive intramolecular forces determining the molecular planarity could help identify new electrochromic materials with altered optical properties.

In addition to the presented electrochromic properties of **TPTTPT**, **TPEEPT**, and **T6**, these oligomeric systems are also promising candidates for new transistor materials. Therefore, we are currently investigating charge-carrier mobilities of these

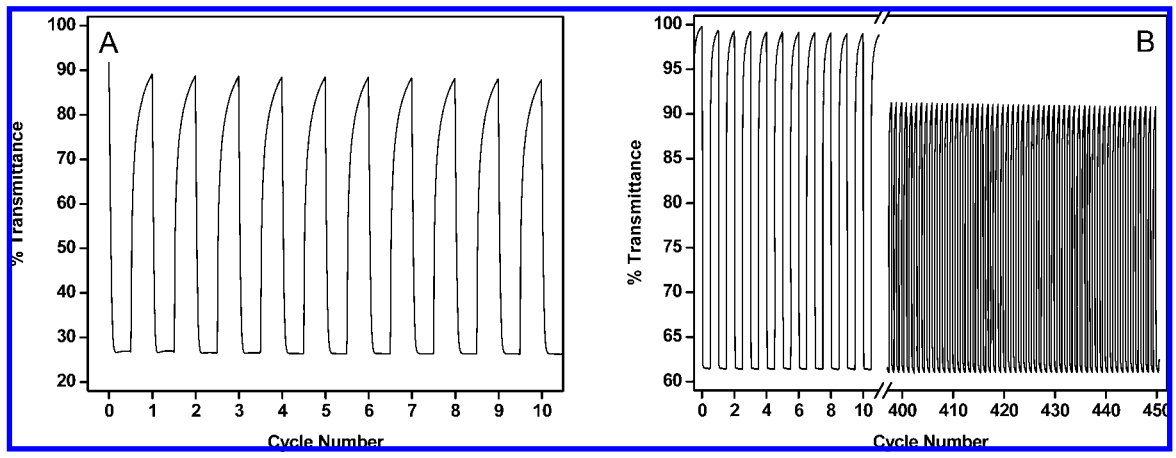

Figure 16. Electrochromic switching of cross-linked **TPEEPT-diacrylate** films (0.1 M tetrabutylammonium perchlorate in dichloromethane) monitored as the percent transmittance (%*T*) at 600 nm with a 30-s delay for each potential (−0.65 and 0.25 V). Ten switching cycles for a 225-nm film (A) and first 10 and last 50 switching cycles for an 85-nm film (B).

oligomers in our laboratories, while also pursuing a deeper understanding of the morphologies of these materials in their solid state.

Acknowledgment. We appreciate funding of this work by the AFOSR (FA9550-06-1-0192) and via a grant to EIC Laboratories (FA9550-05-C-0147). K.A.A. acknowledges the National Science Foundation and the University of Florida for funding the purchase of the X-ray equipment. We thank Geeta Kheter Paul for the supply of compound **10**.

Supporting Information Available: Experimental procedures including full characterization for all new compounds. Cyclic voltammograms showing the scan rate dependence for **TPT-TPT-Me$_2$**, **TPEEPT-Me$_2$**, and **T6-diol**in solution as well as for **TPEEPT-diacrylate** in the solid state. UV−vis spectra displaying the solution oxidation of **T6-diol**. Chronoabsorptometry showing the electrochromic switching of cross-linked **TPEEPT-diacrylate** films. Listings of crystal data and structure refinement parameters, atomic coordinates, bond lengths and angles, anisotropic displacement parameters, hydrogen coordinates, and isotropic displacement parameters for **PTTP** and **PEEP** (PDF and CIF). This material is available free of charge via the Internet at http://pubs.acs.org.

JA7112273